TITLE OF ENTRY

Physical Analogies for Ear Recognition

Handbook of Biometrics, pp 1082-1088

David J. Hurley, Mark S. Nixon
School of Electronics and Computer Science,
University of Southampton,
SO17 1BJ, UK
djh@AnalyticalEngines.co.uk msn@ecs.soton.ac.uk

SYNONYMS

Ear biometrics = Ear Recognition
Force Field Feature Extraction = Field Line Feature Extraction;
Convergence Feature Extraction = Convergence

DEFINITION

Hurley et al [1,2,3] have developed a pair of invertible linear transforms called the **force field transform** and **potential energy transform** which transforms an ear image into a force field by pretending that pixels have a mutual attraction proportional to their intensities and inversely to the square of the distance between them rather like Newton's Law of Universal Gravitation. Underlying this force field there is an associated potential energy field which in the case of an ear takes the form of a smooth surface with a number of peaks joined by ridges. The peaks correspond to potential energy wells and to extend the analogy the ridges correspond to potential energy channels. Since the transform also turns out to be invertible, all of the original information is preserved and since the otherwise smooth surface is modulated by these peaks and ridges, it is argued that much of the information is transferred to these features and that therefore they should make good features. An analysis of the mechanism of this algorithmic **field line feature extraction** approach leads to a more powerful method called **convergence feature extraction** based on the divergence of force direction revealing even more information in the form of anti-wells and anti-channels.

MAIN BODY TEXT

1 Introduction

The last 10 years or so has seen increasing interest in ears as a biometric with signigicant contributions from computer vision researchers [1,2,3,4,5,6,7,8]. In this context we have developed the Force Field Transform which effectively filters an ear image by convolving it with a huge inverse square kernel more than four times the size of the image, the force then being the gradient of the resulting massively smoothed image. Force field feature extraction subsequently exploits the directinonal properties of the force field to automaticlally locate ear features in the form of potential channels and wells. The force field paradigm allows us to draw upon a wealth of proven techniques from vector field calculus; for example we exploit the divergence operator on the force field direction yielding a nonlinear operator which we call convergence of force direction leading to the even more powerfutl convergence feature extration. The extreme kernel size results in the smoothed image having a general dome shape which gives rise to brightness sensitivity issues, but we argue by showing that the field line features are hardly distorted that this will have little overall effect and this conclusion is borne out by including brightness variation in our recognition tests. On the other hand, the dome shape leads to an automatic extraction advantage and this is demonstrated by using deliberately poorly registered and poorly extracted images in recognition tests and then comparing the results with those for PCA (principal component analysis) under the same conditions, where we see that the ear images have to be accurately extracted and registered for PCA to achieve comparable results. The technique is validated by achieving a recognition rate of 99.2% on a set of 252 ear images taken from the XM2VTS face database [10]. Not only is the inherent automatic extraction advantage demonstrated but we also show that it performs even more favourably against PCA under variable brightness conditions, and we also demonstrate its excellent noise performance by showing that noise has little effect on recognition results. Thus we have validated the technique by achieving good ear recognition results, and in the process we have contributed to the mounting evidence that the human ear has considerable biometric value.

2 Ear Feature Extraction

2.1 Force Field Feature Extraction

Here we describe the force field transform and algorithmic field line feature extraction before introducing convergence feature extraction. The mathematical concepts we use can be found in basic works on electromagnetics [9] and a more detailed description of the transform can be found in [3]. We consider faster computation using convolution

and the FFT (Fast Fourier Transform) and also consider the question of brightness sensitivity both theoretically and by demonstration.

The image is first transformed to a force field by treating the pixels as an array of mutually attracting particles that attract each other according to the product of their intensities and inversely to the square of the distances between them. Each pixel is assumed to generate a spherically symmetrical force field so that the total force $\mathbf{F}(\mathbf{r}_j)$ exerted on a pixel of unit intensity at the pixel location with position vector $\mathbf{r}_j$ by a remote pixels with position vector $\mathbf{r}_i$ and pixel intensities $P(\mathbf{r}_i)$ is given by the vector summation,

$$\mathbf{F}(\mathbf{r}_j) = \sum_i \left\{ \begin{array}{c} P(\mathbf{r}_i)\dfrac{\mathbf{r}_i - \mathbf{r}_j}{\left|\mathbf{r}_i - \mathbf{r}_j\right|^3} \forall i \neq j \\ 0 \forall i = j \end{array} \right\} \quad (1)$$

The underlying energy field $E(\mathbf{r}_j)$ is similarly described by,

$$E(\mathbf{r}_j) = \sum_i \left\{ \begin{array}{c} \dfrac{P(\mathbf{r}_i)}{\left|\mathbf{r}_i - \mathbf{r}_j\right|} \forall i \neq j \\ 0 \forall i = j \end{array} \right\} \quad (2)$$

To calculate the force and energy fields for the entire image these calculations should be performed for every pixel but this requires the number of applications of equations 1 and 2 to be proportional to the square of the number of pixels, so for faster calculation the process is treated as a convolution of the image with the force field corresponding to a unit value test pixel, and then invoking the Convolution Theorem to perform the calculation as a frequency domain multiplication, the result of which is then transformed back into the spatial domain. The force field equation for an $M \times N$ pixel image becomes,

$$forcefield = \sqrt{M} \times \sqrt{}\mathfrak{I}^{-1}[\mathfrak{I}(unitforcefield) \times \mathfrak{I}(image)] \quad (3)$$

where $\mathfrak{I}$ stands for the Fourier Transform and $\mathfrak{I}^{-1}$ for its inverse. Figure 1 shows how to implement this in *Mathcad* in which 1**j** denotes the complex operator and **cfft** and **icfft** denote the Fourier and inverse Fourier transforms, respectively. Also, because the technique is based on a natural force field there is the prospect of a hardware implementation in silicon by mapping the image pixels to electric charges, which would lead to very fast real time force field calculation.

```
ff(pic) := | sr ← 2·(rows(pic) − 1), sc ← 2·(cols(pic) − 1)
           | r ← rows(pic) − 1, c ← cols(pic) − 1
           | for rr ∈ 0..sr
           |   for cc ∈ 0..sc
           |     usr_{rr,cc} ← (r + c·j) − (rr + cc·j) / (|r + c·j − (rr + cc·j)|)^3
           | usr_{3·rows(pic)−3, 3·cols(pic)−3} ← 0
           | pic_{3·rows(pic)−3, 3·cols(pic)−3} ← 0
           | oup ← sqrt(rows(pic)·cols(pic)) · icfft((cfft(usr)·cfft(pic)))
           | ff ← submatrix(oup, r, 2·r, c, 2·c)
```

Figure 1 Force field by convolution in Mathcad.

Figure 4(a) demonstrates field line feature extraction for an ear image where a set of 44 test pixels is arranged around the perimeter of the image and allowed to follow the field direction so that their trajectories form field lines which capture the general flow of the force field. The test pixel positions are advanced in increments of one pixel width, and the test pixel locations are maintained as real numbers, producing a smoother trajectory than if they were constrained to occupy exact pixel grid locations. Notice the two obvious potential wells in the lower part of the field.

The effect of brightness change will first be analysed by considering its effect on the energy field and then confirmed by visual experiment. Should the individual pixel intensity be scaled by a factor a and also have and an additive intensity component b, we would have,

$$E(\mathbf{r}_j) = \sum_i \left[\mathbf{r} \quad \mathbf{r} \right] \sum \left[\mathbf{r} \quad \mathbf{r} \right] \sum \left[\mathbf{r} \quad \mathbf{r} \right] \qquad (4)$$

We see that scaling the pixel intensity by the factor a merely scales the energy intensity by the same factor a, whereas adding an offset b is more troublesome, effectively adding a pure energy component corresponding to an image with constant pixel intensity b. The effect of the offset and scaling is shown in Figure Figure 2 with the channels superimposed. We see that scaling by a factor of 10 in (e) has no effect as expected. The original image in (a) has a mean value of 77 and a standard deviation of 47. Images (b) to (d) show the effect of progressively adding offsets of one standard deviation. At one standard deviation the effect is hardly noticeable and even at 3 standard deviations the change is by no means catastrophic as the channel structure alters little. We therefore conclude that operational lighting variation in a controlled biometrics environment will have little effect. These conclusions are borne out by the results of the corresponding recognition experiments in Table 1.

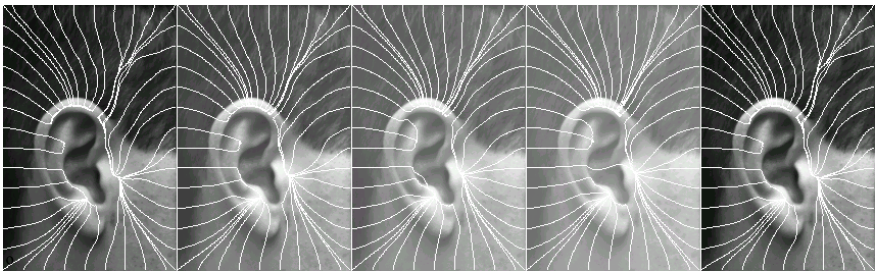

(a) original (b) 1 std. dev. (c) 2 std. devs. (d) 3 std. devs. (e) scaled ×10

Figure 2 Effect of additive and multiplicative brightness changes

2.2 Convergence Feature Extraction

The analytical method came about as a result of analyzing in detail the mechanism of **field line feature extraction**. As shown in Figure 4(d), when the arrows usually used to depict a force field are replaced with unit magnitude arrows, thus modeling the directional behavior of exploratory test pixels, it becomes apparent that channels and wells arise as a result of patterns of arrows converging towards each other, at the interfaces between regions of almost uniform force direction. As this brings to mind the divergence operator of vector calculus, it was natural to investigate the nature of any relationship that might exist between channels and wells and this operator. This resulted not only in the discovery of a close correspondence between the two, but also revealed extra information corresponding to the interfaces between diverging arrows, leading to a more general description of channels and wells in the form of a mathematical function in which wells and channels are revealed to be peaks and ridges respectively in the function value. The new function maps the force field to a scalar field, taking the force as input and returning the additive inverse of the divergence of the force direction. The function will be referred to as the **force direction convergence field** $C(\mathbf{r})$ or just **convergence** for brevity. A more formal definition is given by

$$C(\mathbf{r}) = -\text{div}\,\mathbf{f}(\mathbf{r}) = -\lim_{\Delta A \to 0} \frac{\int \mathbf{f}(\mathbf{r}) \cdot d\mathbf{l}}{\Delta A} = -\nabla \cdot \mathbf{f}(\mathbf{r}) = -\left(\frac{\partial f_x}{\partial x} + \frac{\partial f_y}{\partial y} \right) \tag{12}$$

where $\mathbf{f}(\mathbf{r}) = \dfrac{\mathbf{F}(\mathbf{r})}{|\mathbf{F}(\mathbf{r})|}$, Δ is incremental area, and $d\mathbf{l}$ is its boundary outward normal. This function is real valued and takes negative values as well as positive ones where negative values correspond to force direction divergence. Figure 3 shows a particular implementation of **convergence** in Mathcad where FF represents the force field and DF is the direction field.

$$
C(FF) := \left|\begin{array}{l}
DF \leftarrow \dfrac{\overrightarrow{FF}}{|FF|} \\
\text{for } r \in 1..\text{rows}(DF) - 1 \\
\quad \text{for } c \in 1..\text{cols}(DF) - 1 \\
\quad\quad \left|\begin{array}{l}
dr \leftarrow \text{Re}\left(DF_{r,c}\right) - \text{Re}\left(DF_{r-1,c}\right) \\
dc \leftarrow \text{Im}\left(DF_{r,c}\right) - \text{Im}\left(DF_{r,c-1}\right) \\
C_{r,c} \leftarrow dr + dc
\end{array}\right. \\
-C
\end{array}\right.
$$

Figure 3 Convergence implemented in Mathcad

We must also stress that convergence is non-linear because it is based on force direction rather than force. This nonlinearity means that we are obliged to perform the operations in the order shown; we cannot take the divergence of the force and then divide by the force magnitude. Div(grad/|grad|) ≠ (div grad)/|grad|. This is quite easily illustrated by a simple example using the scalar field e^x in Equation 6,

$$
\left\{\begin{array}{c}\text{div}\left(\text{grad}/|\text{grad}|\right) \\ \nabla\left(\dfrac{\nabla e^x}{|\nabla e^x|}\right) = \nabla\left(\dfrac{e^x \mathbf{i}}{e^x} = \nabla \mathbf{i} = 0\right)\end{array}\right\} \neq \left\{\begin{array}{c}(\text{div grad})/|\text{grad}| \\ \dfrac{\nabla \cdot \nabla e^x}{|\nabla e^x|} = \dfrac{e^x}{e^x} = 1\end{array}\right\} \qquad \textbf{(6)}
$$

where **i** is a unit vector in the *x* direction. This illustrates that even though convergence looks very much like a Laplacian operator, it definitely is not.

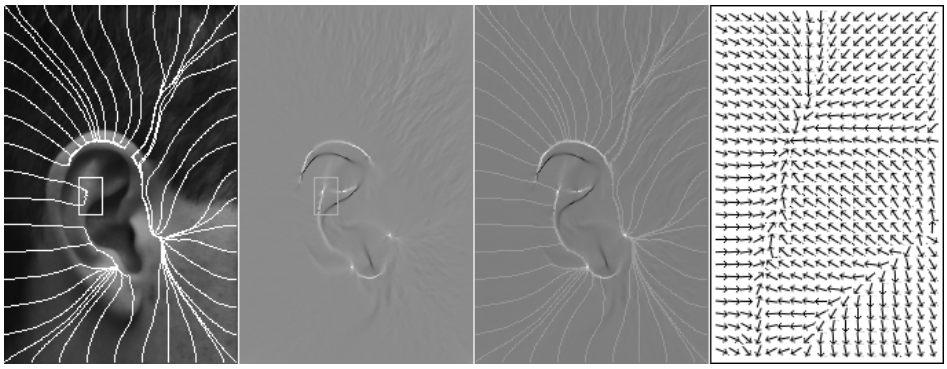

(a) field lines (b) convergence field (c) superimposition (d) force direction

Figure 4 Convergence field

Figure 4 shows the relationship between field lines (a) and convergence (b) by merging the two fields in (c). A small rectangular section of the force direction field indicated by a small rectangular insert in (a) and (b) is shown magnified in (d). We can

see clearly how channels coincide with white convergence ridges and also that wells coincide with convergence peaks which appear as bright spots. Notice the extra information in the center of the convergence map that is not in the field line map. Negative convergence values representing antichannels appear as dark bands, and positive values corresponding to channels appear as white bands. We see that the antichannels are dominated by the channels, and that the antichannels tend to lie within the confines of the channels. Notice also the correspondence between converging arrows and white ridges, and between diverging arrows and black ridges. The features detected tend to form in the center of the field due to its overall dome shape, with channels and wells tending to follow intensity ridges and peaks whereas antichannels and antiwells tend to follow intensity troughs and hollows.

3 Ear Recognition

The technique was validated on a set of 252 ear images taken from 63 subjects selected from the XM2VTS face database [10] by multiplicative template matching of ternary thresholded convergence maps where levels less than minus one standard deviation are mapped to -1, whilst those greater than one standard deviation map to +1, and those remaining map to 0. A threshold level of one standard deviation was chosen experimentally resulting in the template channel thickness shown in Figure 5(c). This figure also shows a rectangular exclusion zone centered on the convergence magnitude centroid; the centroid of the convergence tends to be stable with respect to the ear features and this approach has the added advantage of removing unwanted outliers such as bright spots caused by spectacles. The size of the rectangle was chosen as 71×51 pixels by adjusting its proportions to give a good fit for the majority of the convergence maps. Notice how for image 000-2 which is slightly lower than the other three, that the centroid-centered rectangle has correctly tracked the template downwards.

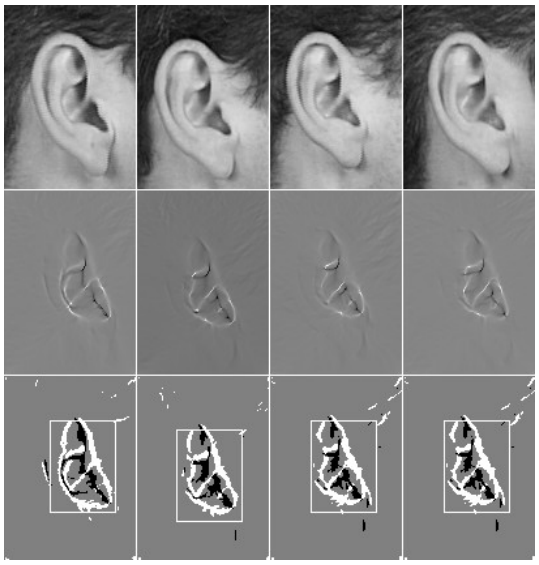

(a) 141×101 Ear images (b) Convergence fields (c) Thresholded convergence maps

Figure 5 Feature extraction for subject 000

The inherent automatic extraction advantage was demonstrated by deliberately not accurately extracting or registering the ears in the sense that the database consists of 141×101 pixel images where the ears have only an average size of 111×73 and are only roughly located by eye in the center of these images. This can be seen clearly in Figure 5(a) where we see a marked variation both in vertical and horizontal ear-location, and also that there is a generous margin surrounding the ears. The force field technique gives a correct classification rate of 99.2% on this set, whereas running PCA [11] on the same set gives a result of only 62.4% but when the ears are accurately extracted by cropping to the average ear size of 111×73, running PCA then gives a result of 98.4%, thus demonstrating the inherent extraction advantage. The first image of the four samples from each of the 63 subjects was used in forming the PCA covariance matrix. Figure 6 shows the first 4 eigenvectors for the 111x73-pixel images. The effect of brightness change by addition was also tested where we see that in the worst case where every odd image is subjected to an addition of 3 standard deviations the force field results only change by 2%. whereas those for PCA under the same conditions fall by 36%, or by 16% for normalized intensity PCA, thus confirming that the technique is robust under variable lighting conditions.

Figure 6 First 4 eigenvectors for 111×73 pixel images

Image type	method	passes	Noise $20\log_{10}$S/N	CCR	bright. add. (std devs.)	decidability
141×101 with deliberately poor extraction and registration	FFE	250/252	Nil	99.2%	0	3.432
	FFE	251/252	18dB	99.6%	0	3.488
	FFE	249/252	12dB	98.8%	0	3.089
	FFE	241/252	6dB	95.6%	0	1.886
	FFE	250/252	Nil	99.2%	1	3.384
	FFE	247/252	Nil	98.0%	2	3.137
	FFE	245/252	Nil	97.2%	3	2.846
	PCA	118/189	Nil	62.4%	0	1.945
111×73 with accurate extraction and registration	PCA	186/189	Nil	98.4%	0	3.774
	PCA	186/189	18dB	98.4%	0	3.743
	PCA	186/189	12dB	98.4%	0	3.685
	PCA	177/189	6dB	93.6%	0	3.606
	PCA	130/189	Nil	68.8%	1	1.694
	PCA	120/189	Nil	63.6%	2	0.878
	PCA	118/189	Nil	62.4%	3	0.476
	PCA	181/189	Nil	95.6%	1 normalized	3.171
	PCA	172/189	Nil	91.0%	2 normalized	1.91
	PCA	166/189	Nil	82.5%	3 normalized	1.14

Table 1 Comparison of force field (FFE) and PCA recognition results

These results are presented in Table 1 where we also include the decidability index after Daugman [12] which combines the mean and standard deviation of the intra-class and inter-class measurement distributions giving a good single indication of the nature of the results. This index d' measures how well separated the distributions are, since recognition errors are caused by their overlap. The measure aims to give the highest scores to distributions with the widest separation between means, and smallest standard deviations. If the two means are $\mu_1$and μ_2 and the two standard deviations are σ and σ_{-} then d' is defined as

$$d' = \frac{|\mu - \iota_{\cdot}|}{\sqrt{(\sigma_{\cdot} + r_{-}^{2})/2}} \tag{7}$$

Notice that the best case index for PCA is slightly higher than the value of 3.43 obtained for the 141×101 images but this could be attributed to the reduction in data set size from 252 to 189 and also to the fact that the images have been more fully extracted for PCA. We have also included noise performance figures where noise has been modeled as additive noise with a zero mean Gaussian distribution The signal to noise ratios of 6dB, 12dB, and 18dB used are calculated as $20\log_{10}(S/N)$. We see that the technique enjoys excellent noise tolerance where even for an extreme noise ratio of 6dB the performance only falls by about 3.6%. Interestingly at a ratio of 18dB the recognition rate actually improves over the noiseless recognition rate, but this must be put down to the combination of small changes and the random nature of the noise process. For reference we have also included the corresponding noise results for PCA under the same conditions, where we see that PCA also performs well under noisy conditions but not quite as well as FFE at 6dB where the fall is about 4.8%.

SUMMARY

In the context of ear biometrics we have developed a linear transform that transforms an ear image, with very powerful smoothing and without loss of information, into a smooth dome shaped surface whose special shape facilitates a novel form of feature extraction that extracts the essential ear signature without the need for explicit ear extraction. We have shown that the technique is robust under variable lighting conditions both by analysis and also by experiment. We have described convergence feature extraction and shown that it is a powerful extension to field line feature extraction. We have validated the technique by experiment where we have shown that it compares favourably with PCA especially under variable lighting conditions. In the process we have contributed to the mounting evidence in support of the recognition potential of the human ear for biometrics.

RELATED ENTRIES

Forensic Evidence of Ears

Holistic Ear Biometrics

Overview of Ear Biometrics

REFERENCES

1. Hurley, D. J., Nixon, M. S. and Carter, J. N., Force Field Energy Functionals for Image Feature Extraction. *Proc. 10th British Machine Vision Conference BMVC99* pp. 604-613, 1999
2. Hurley, D. J., Nixon, M. S. and Carter, J. N., Force Field Energy Functionals for Image Feature Extraction, *Image and Vision Computing*, **20**, pp. 311-317, 2002
3. Hurley, D. J., Nixon, M. S. and Carter, J. N., Force Field Feature Extraction for Ear Biometrics, *Computer Vision and Image Understanding,* 2005, CVIU(98), No. 3, pp. 491-512
4. D. J. Hurley, B. Arbab-Zavar and M. S. Nixon,Handbook of Biometrics – Chapter: The Ear as Biometric, pages 131-150, Springer US, 2008,
5. Burge, M., and Burger, W., Ear biometrics in computer vision, *Proc. ICPR 2000,* pp. 822-826, 2002
6. Yan, P., Bowyer, K. W., Biometric Recognition Using Three-dimensional Ear Shape, *IEEE Transactions on Pattern Analysis and Machine Intelligence* 29 (8), 1297-1308, August 2007.
7. Moreno,B., Sanchez,a., Velez.,J.F., On the Use of Outer Ear Images for Personal Identification in Security Applications, *Proc. IEEE 33rd Annual International Carnahan Conference on Security Technology*, 5-7 Oct. 1999
8. Chen, H., Bhanu, B., "3D free-form object recognition in range images using local surface patches," Pattern Recognition Letters, Vol. 28, No.10, pp. 1252-1262, July 2007.
9. Sadiku, M.N.O., *Elements of Electromagnetics*, Saunders College Publishing, Second Ed., 1989.
10. Messer, K., Matas, J., Kittler, J., Luettin, J., and Maitre, G., XM2VTSDB: The Extended M2VTS Database, *Proc. AVBPA'99* Washington D.C., 1999
11. Turk,M., Pentland,A., Eigenfaces for Recognition, *Journal of Cognitive Neuroscience*, pp.71-86, March 1991
12. Daugman, J., Biometric decision landscapes, *Technical Report TR482*, University of Cambridge Computer Laboratory, 1999

DEFINITIONAL ENTRY

Force Field Transform

An invertible linear transform which transforms an image into a force field by pretending that pixels have a mutual attraction proportional to their intensities and inversely to the square of the distance between them rather like Newton's Law of Universal Gravitation. Each pixel is assumed to generate a spherically symmetrical force field so that the total force $\mathbf{F}(\mathbf{r}_j)$ exerted on a pixel of unit intensity at the pixel location with position vector $\mathbf{r}_j$ by a remote pixels with position vector $\mathbf{r}_i$ and pixel intensities $P(\mathbf{r}_i)$ is given by the vector summation,

$$\mathbf{F}(\mathbf{r}_j) = \sum_i \left\{ \begin{array}{c} P(\mathbf{r}_i) \dfrac{\mathbf{r}_i - \mathbf{r}_j}{\left|\mathbf{r}_i - \mathbf{r}_j\right|^3} \forall i \neq j \\ 0 \forall i = j \end{array} \right\} \quad (8)$$

In order to calculate the force field for the entire image, this equation should be applied at every pixel position in the image. In practice this computation would be done in the frequency domain using Equation 9 where $\Im$ stands for FFT and $\Im$ stands for inverse FFT.

$$forcefield = \sqrt{M} \times \Im^{-1} \left[\Im \left[unit\ forcefield \right] \times \Im \left[image \right] \right] \quad (9)$$

For a more detailed explanation see **physical analogies for ear recognition**.

DEFINITIONAL ENTRY

Potential Energy Transform

An invertible linear transform which transforms an image into an energy field by treating the pixels as an array of particles that act as the source of a Gaussian potential energy field. It is assumed that there is a spherically symmetrical potential energy field generated by each pixel, so that $E(\mathbf{r}_j)$ is the total potential energy imparted to a pixel of unit intensity at the pixel location with position vector $\mathbf{r}_j$ by the energy fields of remote pixels with position vectors $\mathbf{r}_i$ and pixel intensities $P(\mathbf{r}_i)$, and is given by the scalar summation,

$$E(\mathbf{r}_j) = \sum_i \left\{ \begin{array}{c} \dfrac{P(\mathbf{r}_i)}{|\mathbf{r}_i - \mathbf{r}_j|} \forall i \neq j \\ 0 \forall i = j \end{array} \right\} \quad \textbf{(10)}$$

To calculate the energy field for the entire image Equation 10 should be applied at every pixel position. For efficiency this is actually calculated in the frequency domain using Equation 11 where $\mathfrak{I}$ stands for FFT and $\mathfrak{I}$ stands for inverse FFT.

$$energyfield = \sqrt{M} \times \mathfrak{I}^{-1}\{\mathfrak{I}(unit\ energyfield) \times \mathfrak{I}(image)\} \quad \textbf{(11)}$$

For a more detailed explanation see **physical analogies for ear recognition**.

DEFINITIONAL ENTRY

Force Field Feature Extraction

The overall objective in defining feature space is to reduce the dimensionality of the original pattern space, whilst maintaining discriminatory power for classification. To meet this objective in the context of ear biometrics a novel force field transformation has been developed which treats the image as an array of mutually attracting particles that act as the source of a Gaussian force field. Underlying the force field there is a scalar potential energy field, which in the case of an ear takes the form of a smooth surface that resembles a small mountain with a number of peaks joined by ridges. The peaks correspond to potential energy wells and to extend the analogy the ridges correspond to potential energy channels. Since the transform also turns out to be invertible, and since the surface is otherwise smooth, information theory suggests that much of the information is transferred to these features, thus confirming their efficacy. Force field feature extraction, using an algorithm similar to gradient descent, exploits the directional properties of the force field to automatically locate these channels and wells, which then form the basis of the characteristic ear features. For a more detailed explanation see **physical analogies for ear recognition**.

DEFINITIONAL ENTRY

Convergence Feature Extraction

Convergence provides a more general description of channels and wells than force field feature extraction. It takes the form of a mathematical function in which wells and channels are revealed to be peaks and ridges, respectively in the function value. This function maps the force field **F**(**r**) to a scalar field *C*(**r**), taking the force as input, and returning the additive inverse of the divergence of the force direction, and is defined by,

$$C(\mathbf{r}) = -\text{div}\,\mathbf{f}(\mathbf{r}) = -\lim_{\Delta A \to 0} \frac{\int \mathbf{f}(\mathbf{r}) \cdot d\mathbf{l}}{\Delta A} = -\nabla \mathbf{f}(\mathbf{r}) = -\left(\frac{\partial f_x}{\partial x} + \frac{\partial f_y}{\partial y} \right) \quad \textbf{(5)}$$

where $\mathbf{f}(\mathbf{r}) = \frac{\mathbf{F}(\mathbf{r})}{|\mathbf{F}(\mathbf{r})|}$ is the force direction, Δ is incremental area, and $d\mathbf{l}$ is its boundary outward normal. This function is real valued and takes negative values as well as positive ones where negative values correspond to force direction divergence. Note that the function is non-linear because it is based on force direction and therefore must be calculated in the given order. For a more detailed explanation see **physical analogies for ear recognition**.